1000 A

UNCLASSIFIED

NRL Report 8380
Copy No. 20 of 70 Copies

Target Identification By First-Pulse Deconvolution

WERNER G. NEUBAUER

Acoustics Division

February 29, 1980

NAVAL RESEARCH LABORATORY
Washington, D.C.

UNCLASSIFIED

[redacted]

[redacted]

SECURITY CLASSIFICATION OF THIS PAGE *(When Data Entered)*

REPORT DOCUMENTATION PAGE		READ INSTRUCTIONS BEFORE COMPLETING FORM
1. REPORT NUMBER NRL REPORT 8380	2. GOVT ACCESSION NO.	3. RECIPIENT'S CATALOG NUMBER
4. TITLE *(and Subtitle)* TARGET IDENTIFICATION BY FIRST-PULSE DECONVOLUTION [redacted]		5. TYPE OF REPORT & PERIOD COVERED Interim report on a continuing NRL problem 6. PERFORMING ORG. REPORT NUMBER
7. AUTHOR(s) Werner G. Neubauer		8. CONTRACT OR GRANT NUMBER(s)
9. PERFORMING ORGANIZATION NAME AND ADDRESS Naval Research Laboratory Washington, DC 20375		10. PROGRAM ELEMENT, PROJECT, TASK AREA & WORK UNIT NUMBERS NRL Problem 81-0357-0
11. CONTROLLING OFFICE NAME AND ADDRESS Naval Material Command MAT 08T214 Washington, DC 20360		12. REPORT DATE February 29, 1980 13. NUMBER OF PAGES 34
14. MONITORING AGENCY NAME & ADDRESS*(if different from Controlling Office)*		15. SECURITY CLASS. *(of this report)* [redacted] 15a. DECLASSIFICATION/DOWNGRADING SCHEDULE Class. by multiple sources. Revw: 30 Nov 1994
16. DISTRIBUTION STATEMENT *(of this Report)* [redacted]		
17. DISTRIBUTION STATEMENT *(of the abstract entered in Block 20, if different from Report)*		
18. SUPPLEMENTARY NOTES [redacted]		
19. KEY WORDS *(Continue on reverse side if necessary and identify by block number)* Acoustic scattering Submarines Echoes Target characteristics		

20. ABSTRACT *(Continue on reverse side if necessary and identify by block number)*

[redacted] A reliable method for identifying an echo by using only the first part of that echo returned by a smooth reflecting body is presented. Dividing the Fourier transform of the entire reflected echo by the Fourier transform of the incident pulse results in a function that is highly variable with frequency. Using only the very first portion of the target echo in this deconvolution process consistently results in a function that changes slowly over the frequency band for a variety of target conditions. This result is demonstrated for echoes reflected from submarine models in air and water. Also, both single-hull (U.S.) and double-hull (Soviet) configurations were

(Continued)

DD FORM 1 JAN 73 1473 EDITION OF 1 NOV 65 IS OBSOLETE
S/N 0102-014-6601

[redacted]

SECURITY CLASSIFICATION OF THIS PAGE *(When Data Entered)*

 [redacted]

ABSTRACT (Continued)

measured in water. Echo results were compared for a coated and uncoated double-hull target. An equivalent full-scale frequency range of between approximately 600 Hz and 1400 Hz was examined. A stable and smooth function of frequency was observed in all cases when the very first part of the reflected pulse was used.

TARGET IDENTIFICATION BY FIRST-PULSE DECONVOLUTION

Pulses specularly reflected from smooth bodies of regular shape are replicas of the incident pulse. They have the same phase if the target may be considered rigid, which is the case for a solid in air, and they are reversed in phase from the incident pulse if the target is acoustically soft (a pressure-release target), such as a bubble in water. The reflection amplitude of the backscattered acoustic far-field pressure is described by a form function $|f_\infty(ka)|$ which is plotted against the variable ka, where k is $2\pi/\lambda$. Here λ is the incident acoustic wavelength and a is the characteristic dimension of a body such as the radius of a sphere. The form function is related to the incident acoustic pressure amplitude $|p_i(t)|$ and the reflected pressure amplitude $|p_r(t)|$ by the equation

$$|p_r(t)| = |p_i(t)|\frac{2a}{r}|f_\infty(ka)|. \tag{1}$$

Here a is the sphere radius and r is the distance from the reflector to the receiver. The form function for a hard (inelastic) and a soft (pressure-release) sphere is shown in Fig. 1. That function is compared for three shapes in Fig. 2 for small values of ka. Prolate spheroid end-on and beam or side-on reflection is described in Fig. 3 by experimentally determined curves. In all cases the curves are smooth curves that vary slowly over a range of ka which may be interpreted as frequency for a fixed size of object (constant a) ; that is, $2\pi/\lambda = 2\pi f/c$, where c is the speed of sound in water (a constant). Also, each curve is different and discloses the geometry of the reflecting object.

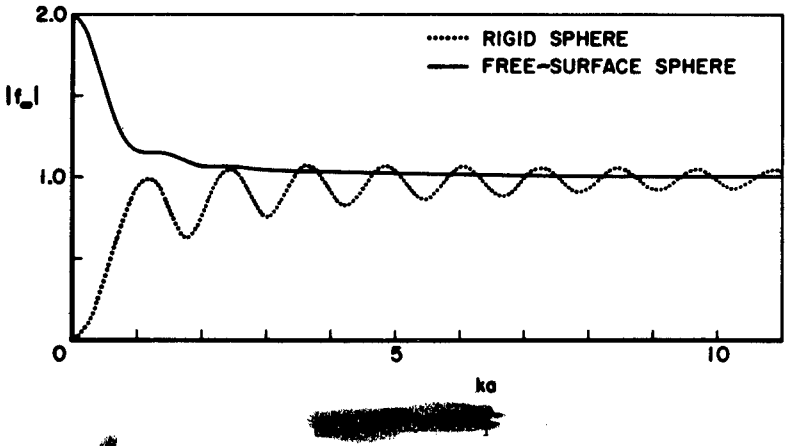

Fig. 1 — Theoretical form function for a rigid sphere and a soft sphere

Manuscript submitted October 26, 1979.

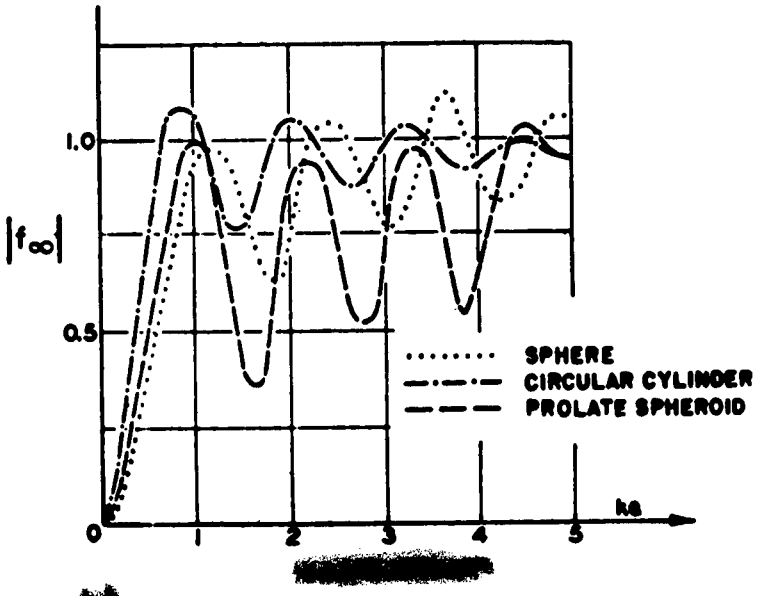

Fig. 2 — Theoretical form function for a sphere (repeated from Fig. 1), a cylinder, and an end-on spheroid

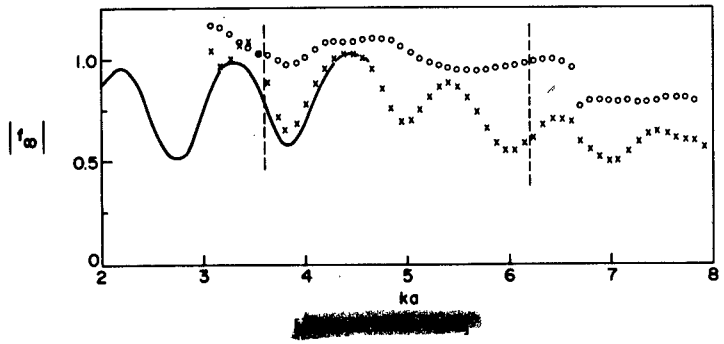

Fig. 3 — Experimentally measured form function for an end-on (×) and beam-on (○) prolate spheriod. The solid curve is the theoretical curve (repeated from Fig. 2). The beam-on set of data is displaced upward to avoid clutter in the plot.

It has been shown [1] that the same (form) function can be otherwise arrived at by deconvolution of the Fourier transforms of the incident and reflected pulses, which are time functions. That is,

$$|f_\infty(ka)| = \frac{2a}{r}\left|\frac{g_r(ka)}{g_i(ka)}\right|, \tag{2}$$

where $g_r(ka)$ is the Fourier transform of the reflected pulse $p_r(t)$ and $g_i(ka)$ is similarly the Fourier transform of the pulse $p_i(t)$ incident on the target. Equation (2) states that the form function is directly proportional to the ratio of the spectrum $|g_r(ka)|$ of the reflected pulse to the spectrum $|g_i(ka)|$ of the incident pulse. The proportionality constant contains only geometric factors for simple geometric shapes and in the case of the sphere is the ratio of the diameter 2a to the range from the receiver to the target.

If appendages are disregarded, submarines are roughly cylinders approximately 10 times as long as they are in diameter and have been regarded so by past calculations [2]. In a more refined sense a submarine could be regarded as a prolate spheroid of approximately a 10:1 major-to-minor axis ratio. For a submarine 9.14 m (30 ft) in diameter a *ka* of 5 corresponds to a frequency of 250 Hz and a *ka* interval of unity corresponds to a frequency internal of 50 Hz for an acoustic wave in water. If an acoustic echo from a submarine is the result of the interaction of acoustic energy with the hull shape and not to a large degree the hull elasticity, the reflection could have the property of varying slowly in amplitude with frequency, as was described for reflections from cylindrical, spherical, and spheriodal geometries (Figs. 1,2, and 3).

In an earlier study [3] reflection of acoustic echoes from a submarine model target in air was measured and, in part, showed that the target had three predominant echo sources: hull, sail, and tail. Measurements were made at a frequency corresponding to a full-scale frequency on a real target of 900 Hz. The sequence of echoes at fixed angles in the forward quadrant of the submarine model for a single incident echo are shown in Fig. 4. The amplitudes of the echoes are separately plotted in Figs. 5b, 5c, and 5d so that they may be compared with the long-pulse-echo return plotted in Fig. 5a, which includes the net echo level when contributions from all three echo sources add together (or subtract) in the phase appropriate to their relative range from the acoustic source and receiver. The hull function (Fig. 5b) can be derived from a distinct echo over a large part of the total target aspect. The exception occurs at and near 180 ° aspect when the first pulse comes from the complex structure of the tail.

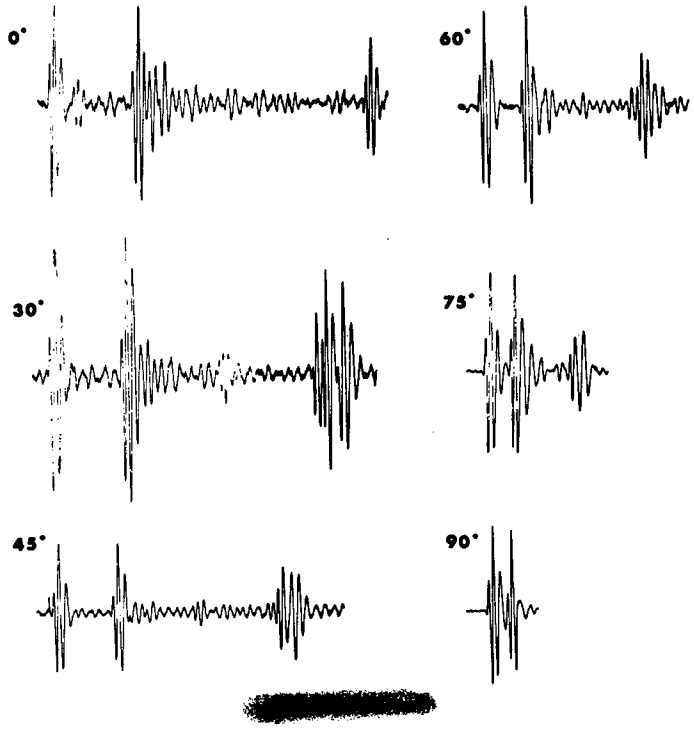

Fig. 4 — Pulse returns at selected angles between bow aspect (0°) and beam aspect from the submarine model used in an earlier study [3] in air at an equivalent-full-scale frequency of 864 Hz

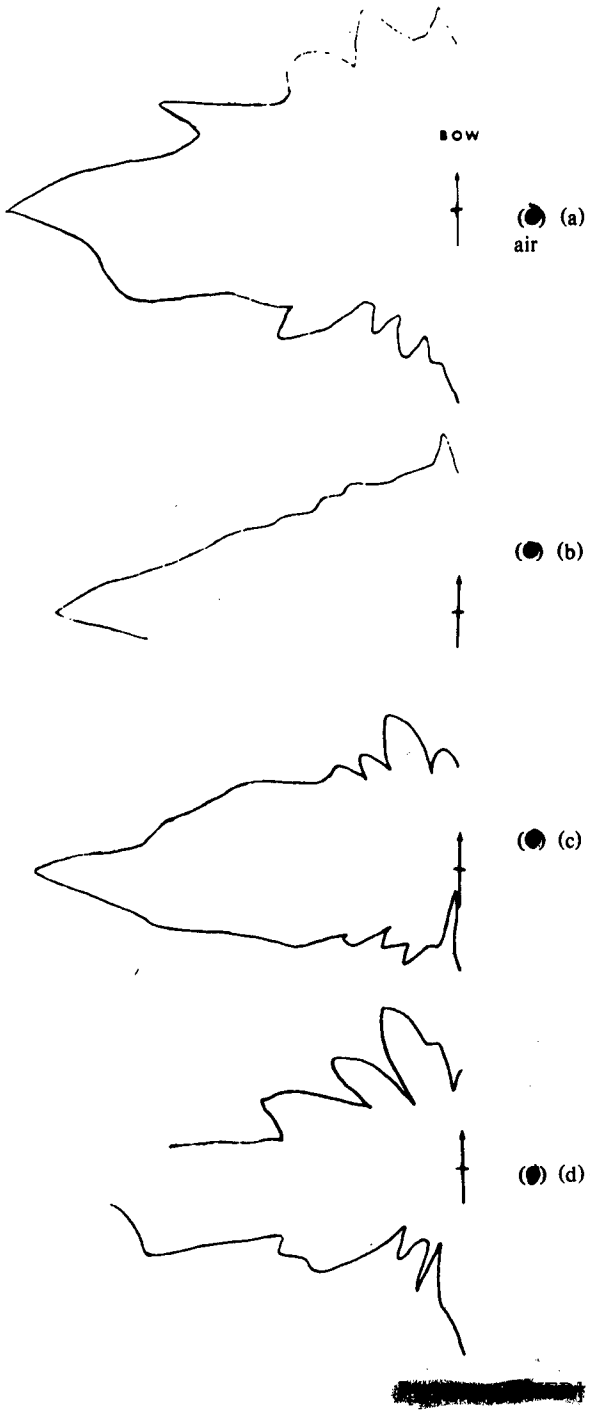

(a) Derived from the whole-model return in air

(b) Derived from the hull return

(c) Derived from the sail return

(d) Derived from the tail return

Fig. 5 — Peak target strength (determined by the amplitudes of the pulses represented in Fig. 4) as a function of aspect

One would reasonably expect the form function derived in the manner of Eq. (2) from the pulse reflected by the hull to be a smooth simple function of ka (or frequency), perhaps slowly oscillating in ka similar to the form functions of Figs. 1, 2, and 3.

The acoustic echo reflected from a submarine model suspended in air is shown in Fig. 6 at an aspect angle of 60° (the bow aspect is 0°). The incident pulse $p_i(t)$, which has a center frequency of 40 kHz (equivalent-full-scale frequency), is shown in Fig. 7. The submarine model is 33 cm (13 in.) long and is a hollow-metallic-shell model of the Skipjack. Experimental measurements are made at low equivalent-full-scale frequencies below 600 Hz, and the air facility accommodates the same models used in underwater measurements. The precision of the air facility was developed and demonstrated for basic studies for reflection from simple shapes [1]. The spectrum $|g_i(ka)|$ of the incident pulse is shown in Fig. 8, and spectra $|g_r(ka)|$ of pulses reflected at aspect angles of 0° (bow), 30° , 60°, and 90° (beam) are shown in Figs. 9a, 10a, 11a, and 12a. Respective deconvolutions performed by fast-Fourier-transform (FFT) techniques are given in Figs. 9b, 10b, 11b, and 12b. The form functions at aspect angles in the forward quadrant are indeed simple slowly varying functions, as anticipated, because of the near satisfaction of the target boundary condition of rigidity, causing the sound in air not to couple well to the relatively solid (relative to air) material of the target and set it into elastic vibration.

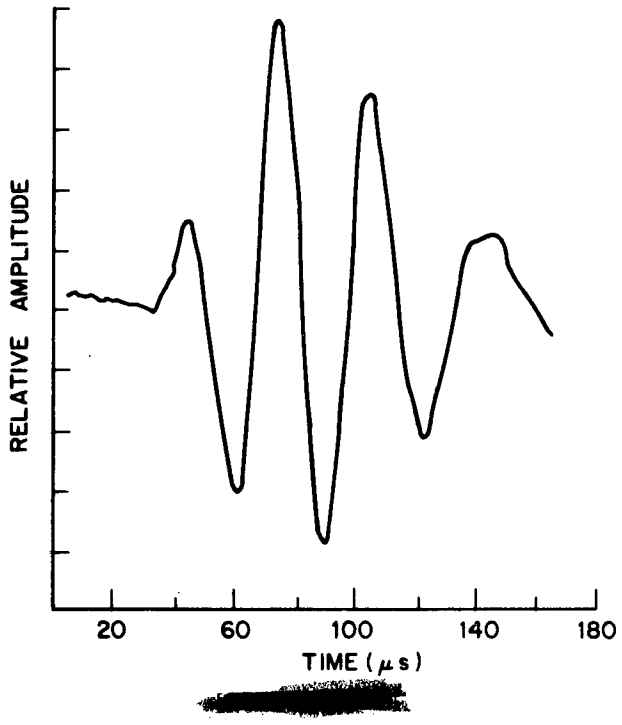

Fig. 6 — The reflected acoustic pulse $Pr(t)$ in air from a submarine model at an aspect angle of 60° from the bow at an equivalent-full-scale frequency of approximately 1 kHz

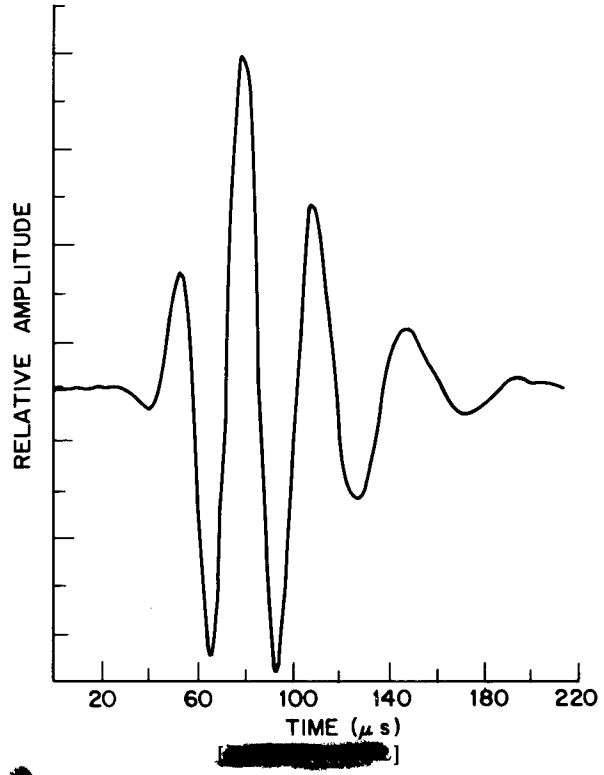

Fig. 7 — The acoustic pulse $p_i(t)$ incident in air on the submarine model that reflected the pulse shown in Fig. 6

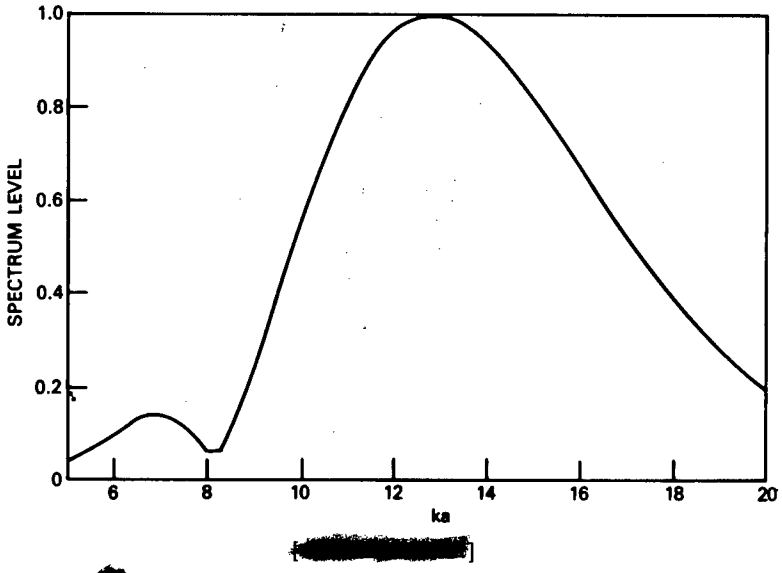

Fig. 8 — The spectrum $|g_i(ka)|$ of the incident pulse in air shown in Fig. 7

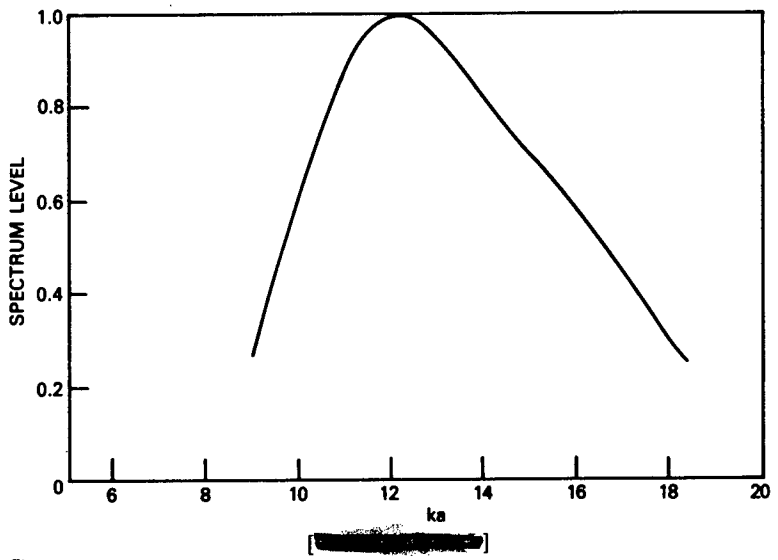

Fig. 9a — the spectrum $|g_r(ka)|$ of the reflected pulse at an aspect angle of 0° in air when the pulse in Fig. 7 is incident on the submarine model

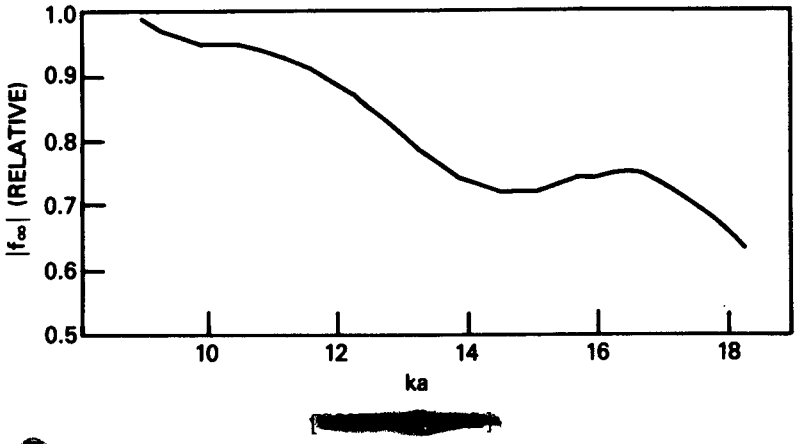

Fig. 9b — The form function resulting from deconvolution (the calculation per Eq. (2)) using the Fourier transform (spectrum) of the reflected pulse's at an aspect angle of 0° in air (Fig. 9a) and the incident pulses Fourier transform (Fig. 8)

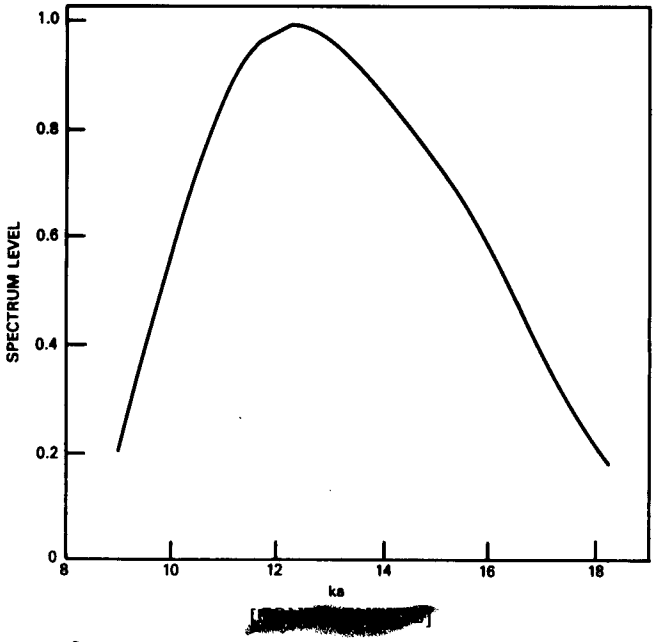

Fig. 10a — The spectrum $|g_r(ka)|$ of the reflected pulse at an aspect angle of 30° in air

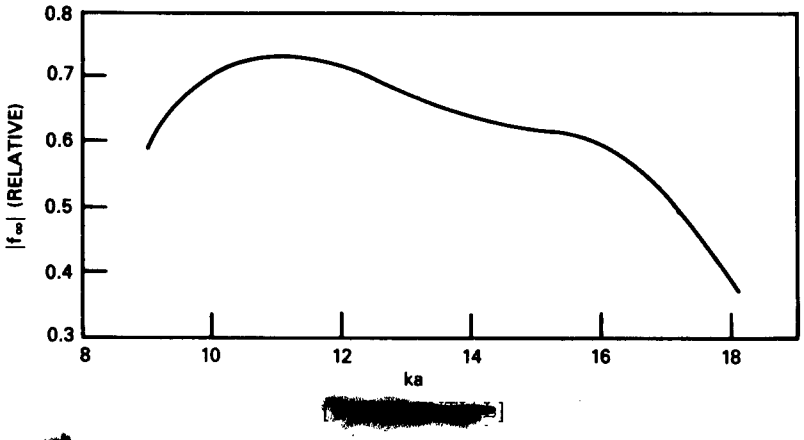

Fig. 10b — The form function resulting from deconvolution using the spectrum of the reflected pulse at an aspect angle of 30°

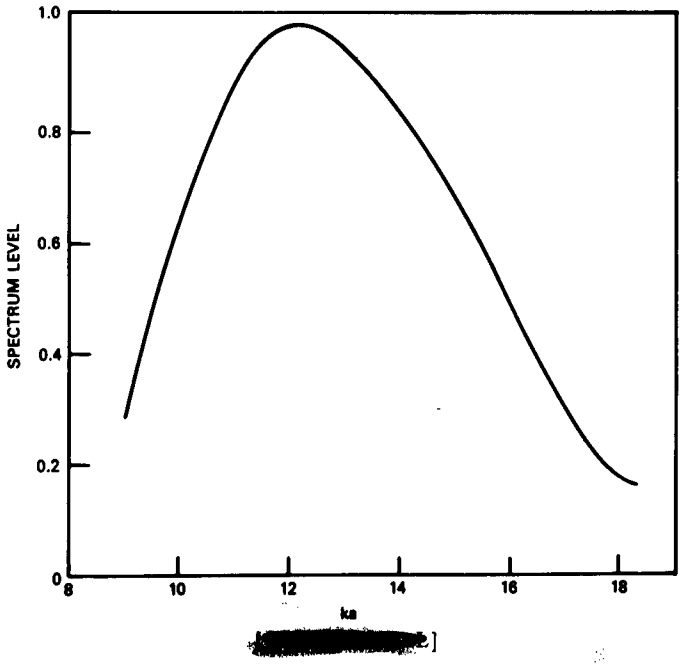

Fig. 11a — The spectrum $|g_r(ka)|$ at an aspect angle of 60° in air

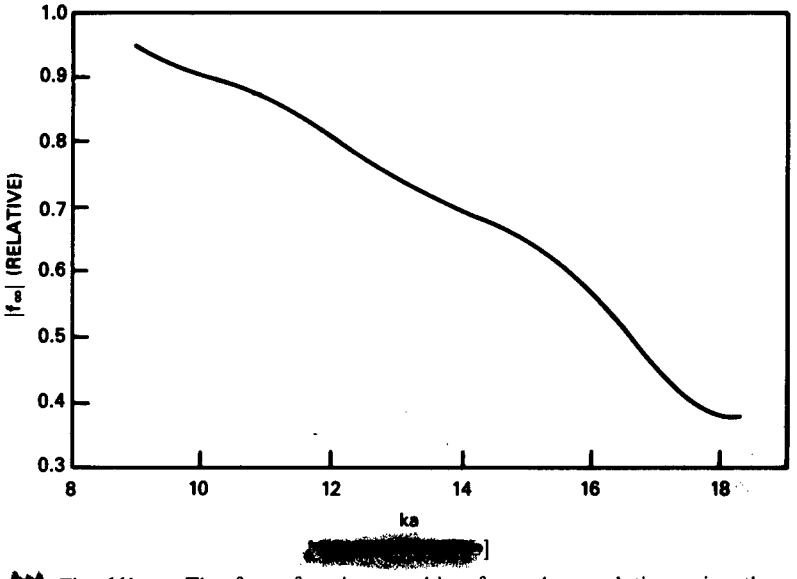

Fig. 11b — The form function resulting from deconvolution using the spectrum of the reflected pulse at an apsect angle of 60°

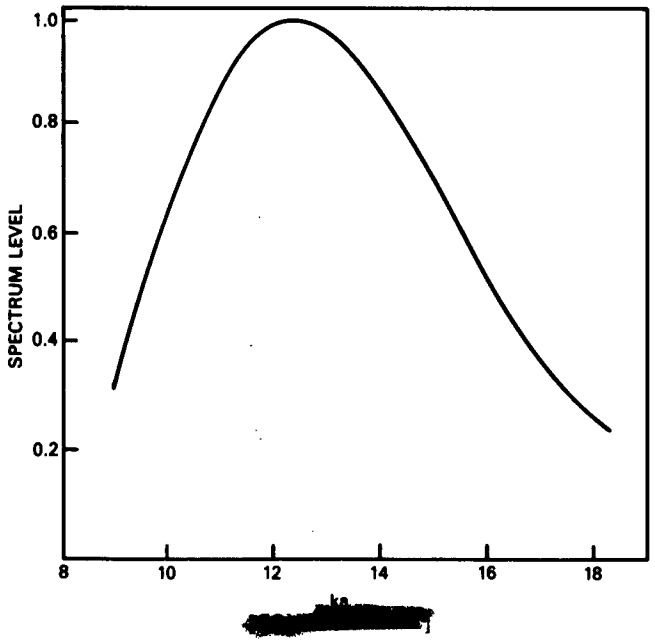

Fig. 12a — The spectrum $|g_r(ka)|$ of the reflected pulse at an aspect angle of 90° in air

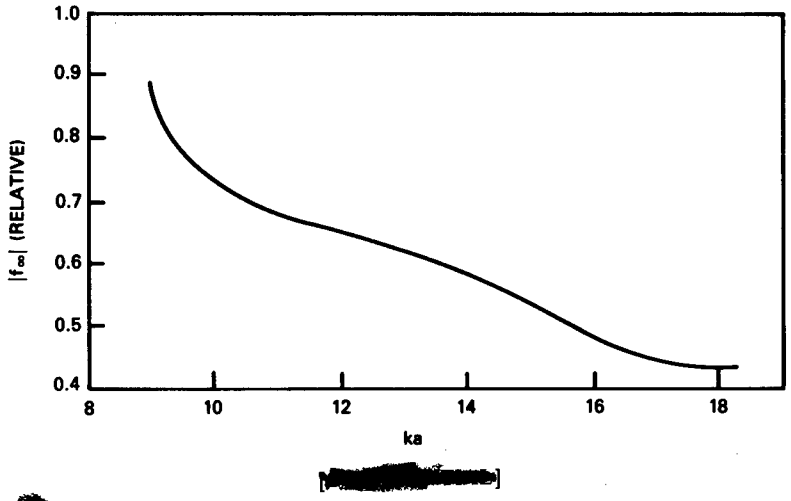

Fig. 12b — The form function resulting from deconvolution using the spectrum of the reflected pulse at an aspect angle of 90°

The same target was next placed in the 570–m^3 (150,000-gal) acoustic pool at NRL, and experiments were performed in water similar to those which were performed in the air echo range. The incident pulse that was used in these water experiments is shown in Fig. 13. The center frequency is 210 kHz, chosen so that the *ka* for the water case would not be far removed from that for the air case and the frequency be one previously used in reflection measurements in water from other bodies. Even though the time scale of the incident pulse at 40 kHz in air in Fig. 7 is different from that of the incident pulse that is used in water and shown in Fig. 13, the characteristic difference in the problem in each medium is apparent from the pulses. In air, short pulses of only a few cycles are relatively easy to achieve at reasonable amplitudes. Transducers (speakers) tend to be relatively broadband. In water, transducers which have a high output tend to be relatively narrow band and ring extensively, causing pulses of many cycles to be typical. Thus, a relatively narrow frequency (*ka*) range is examined in experiments in water, and the pulse that reflects from the very first part of the target is likely to not have ceased before an additional reflector contributes to the echo. That is, pulse isolation of various contributors is more difficult in water. In addition, in water the acoustical energy is better coupled to the target material because of the more nearly equal relative acoustic impedance of water and the target material, which is copper in this case. So in water elastic participation of the target is hard to avoid. However, the best chance to do so is to use the very first part of the echo in a time interval only as long as the incident pulse.

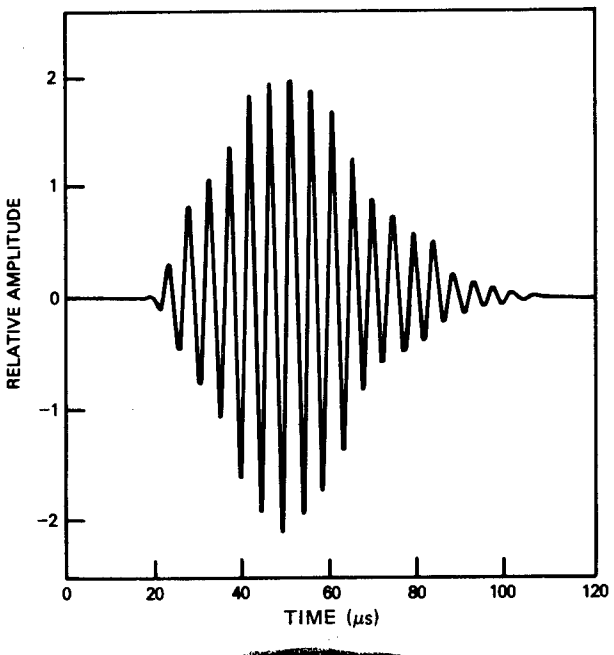

Fig. 13 — The acoustic pulse $p_i(t)$ incident on the submarine model in water

(●) The spectrum $|g_i(ka)|$ of the incident pulse (Fig. 13) is given in Fig. 14. Division of the spectrum of the entire reflected signal $|g_r(ka)|$, given in Fig. 15a by the spectrum of the incident pulse $|g_i(ka)|$ given in Fig. 14 results in the magnitude of the form function $|f_\infty(ka)|$ given in Fig. 15b. Here the vertical scale is in arbitrary linear units. The center equivalent-full-scale frequency of the incident pulse for a comparable real-submarine case would be 576 Hz. Similar spectra and form functions resulting from deconvolution with the incident pulse spectra are given in Figs. 16 and 17 for aspect angles of 40° and 50° respectively. The curves do bear a similarity to each other but are highly irregular complicated curves.

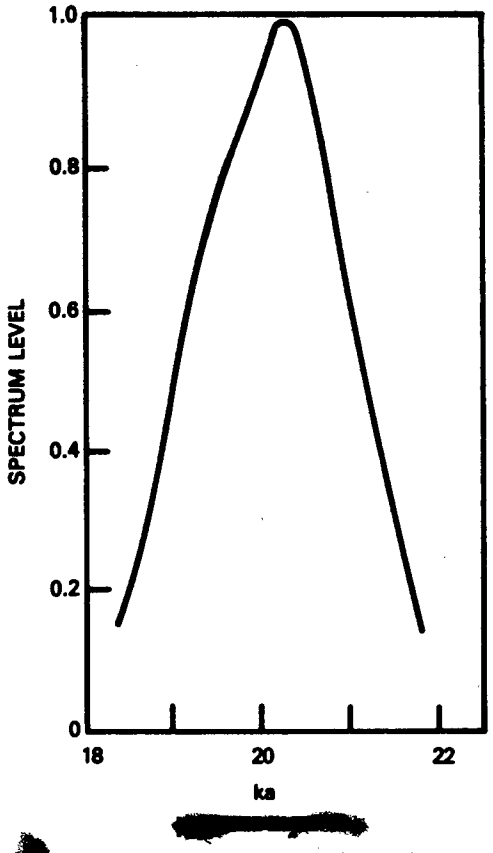

Fig. 14 — The spectrum $|g_i(ka)|$ of the incident pulse in water shown in Fig. 13

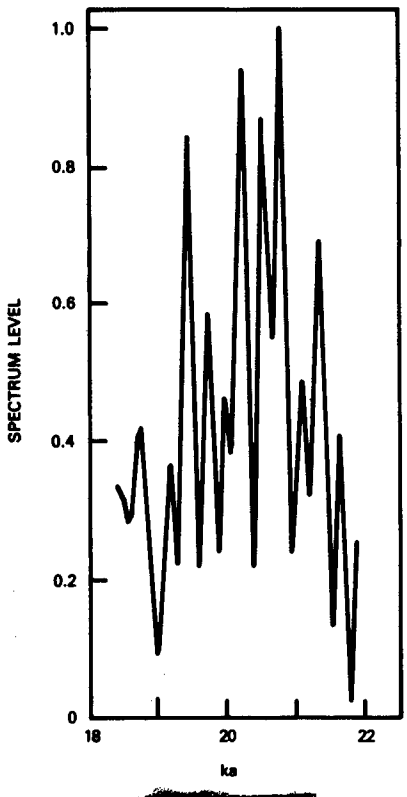

Fig. 15a — The spectrum $|g_r(ka)|$ of the entire reflected pulse at an aspect angle of 30° in water when the pulse in Fig. 13 is incident on the submarine model

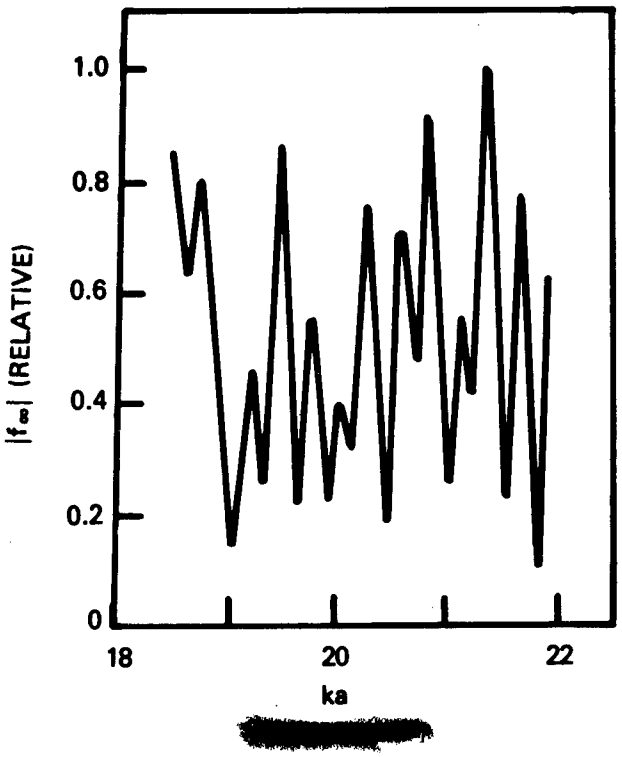

Fig. 15b — The form function resulting from deconvolution using the spectrum of the entire reflected pulse at an aspect angle of 30° in water

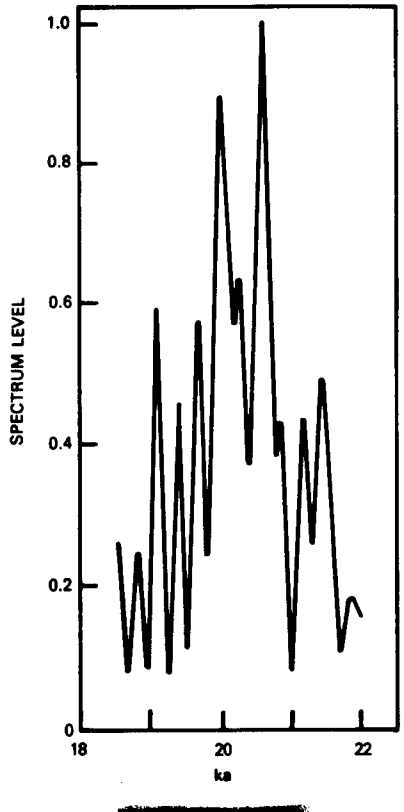

Fig. 16a — The spectrum $|g_r(ka)|$ of the entire reflected pulse at an aspect of 40° in water

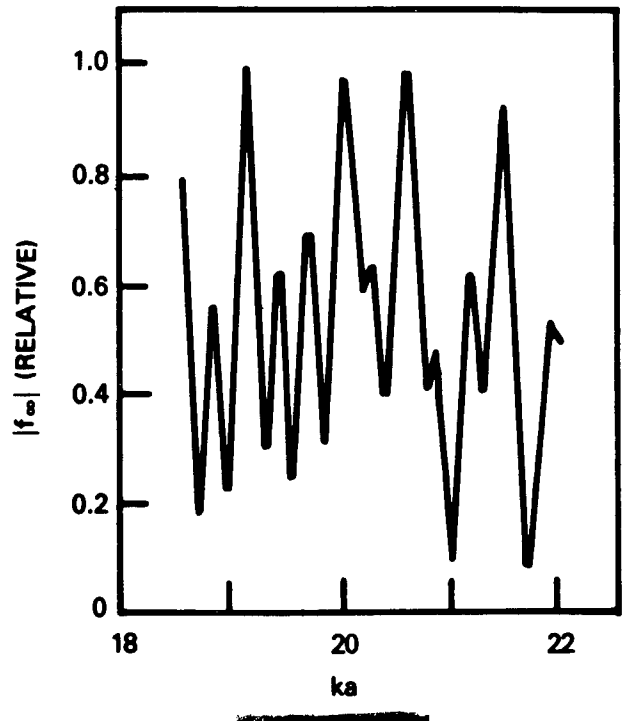

Fig. 16b — The form function resulting from deconvolution using the spectrum of the entire reflected pulse at an aspect angle of 40° in water

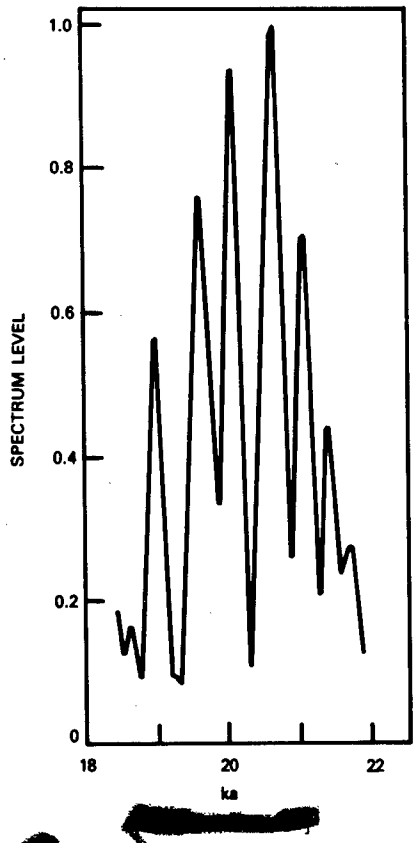

Fig. 17a — The spectrum $|g_r(ka)|$ of the entire reflected pulse at an aspect angle of 50° in water

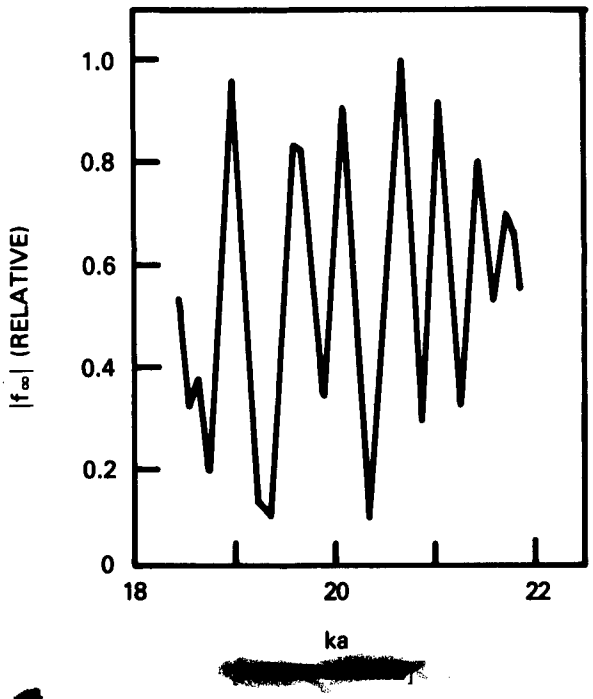

Fig. 17b — The form function resulting from deconvolution using the spectrum of the entire reflected pulse at an aspect angle of 50° in water

If, on the other hand, only the very first part of the reflected pulse is used in the procedure to arrive at spectrum for the reflected pulse, then for 0° (bow aspect) the transform shown in Fig. 18a is derived for and the comparable form function shown in Fig. 18b is derived. Similar spectra and form functions similarly derived from experimentally measured pulses in water are shown in Figs. 19, 20, 21, 22, and 23 for aspect angles of 30°, 40°, 50°, 60°, and 80° respectively. The reflected pulse at an aspect of 30° is shown in Fig. 24. A repeat of the data taken at 30° and 40° two weeks later is shown in Figs. 25 and 26, and comparison with the earlier data in Figs. 19 and 20 shows the variation and stability of the function that may be expected. The resulting form functions are found to be smooth slowly varying functions that bear a similarity to each other and those of simple geometries shown earlier.

The Skipjack submarine model measured in air and water was a single-hull model and had no internal structure. The existence of such internal structure or a drastically different hull configuration could modify the conclusions one might draw from the acoustical measurements made in water on the Skipjack model. Another modifying influence could be the presence of an echo-modifying coating on the target submarine. The next series of experiments were designed to test the validity of a similar conclusion: that a simple smooth form function could be derived from the "first" echo using a significantly different hull configuration, a double-hulled submarine, as well as using such a submarine covered with an echo-reduction coating.

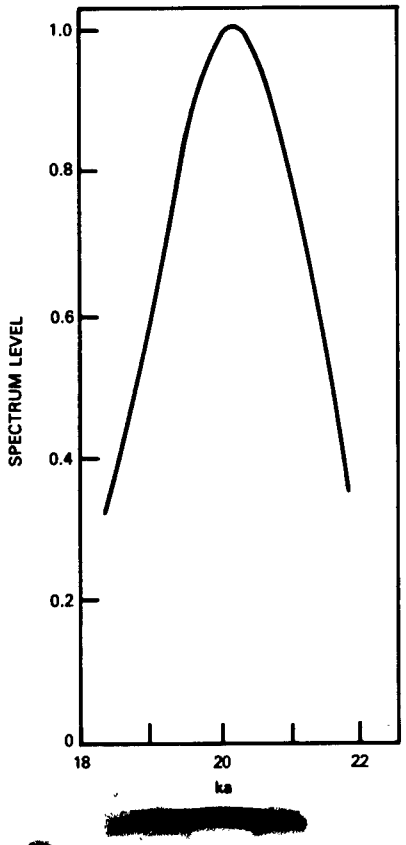

Fig. 18a — The spectrum $|g_r(ka)|$ of the first pulse reflected at an aspect angle of 0° in water when the pulse in Fig. 13 is incident on the submarine model

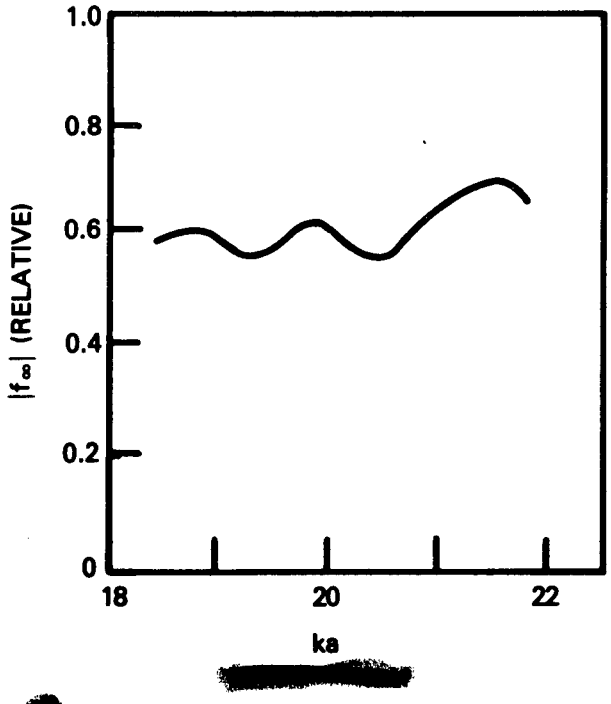

Fig. 18b — The form function resulting from deconvolution using the spectrum of only the first pulse reflected at an aspect angle of 0° in water (Fig. 18a) and the spectrum of the incident pulse (Fig. 14)

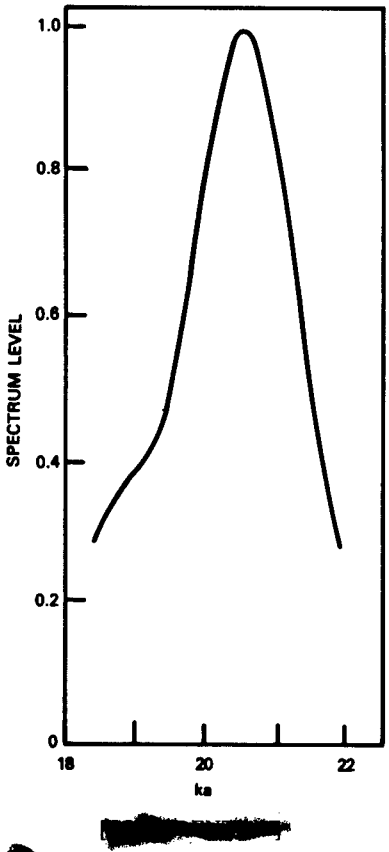

Fig. 19a — The spectrum $|g_r(ka)|$ of the first pulse reflected at an aspect angle of 30° in water

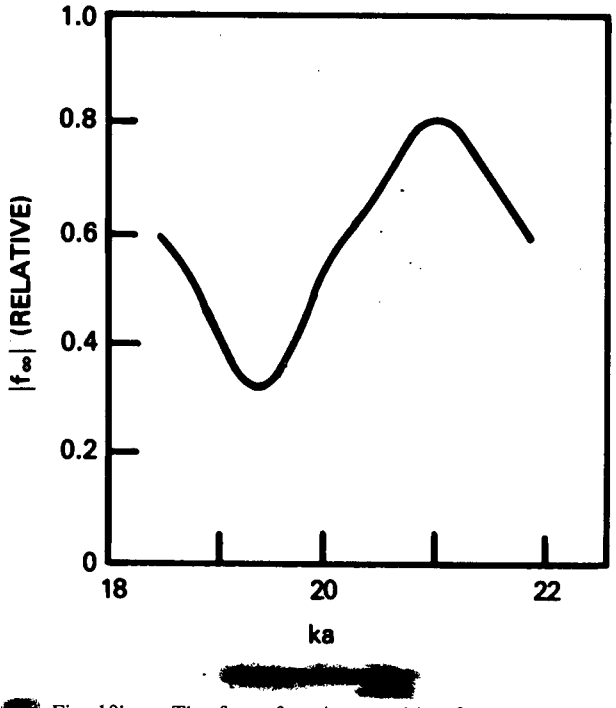

Fig. 19b — The form function resulting from deconvolution using the spectrum of only the first pulse reflected at an aspect angle of 30° in water

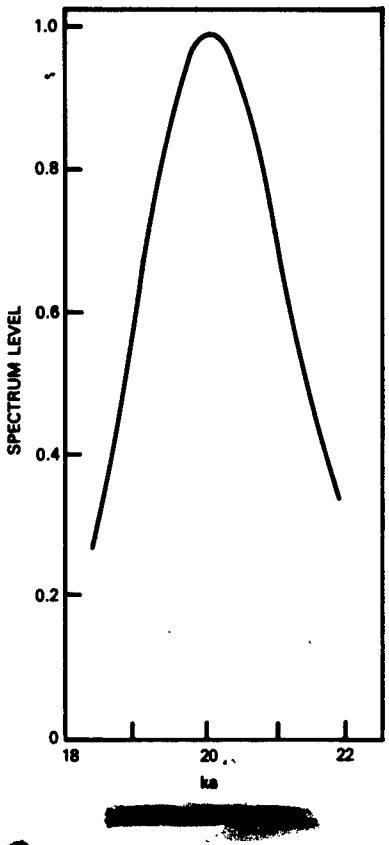

Fig. 20a — The spectrum $|g_r(ka)|$ of the first pulse reflected at an aspect angle of 40° in water

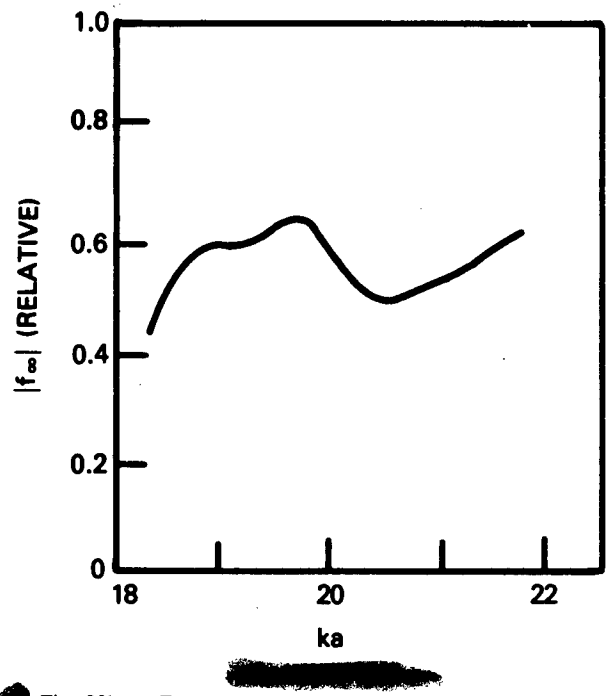

Fig. 20b — The form function resulting from deconvolution using the spectrum of only the first pulse reflected at an aspect angle of 40° in water

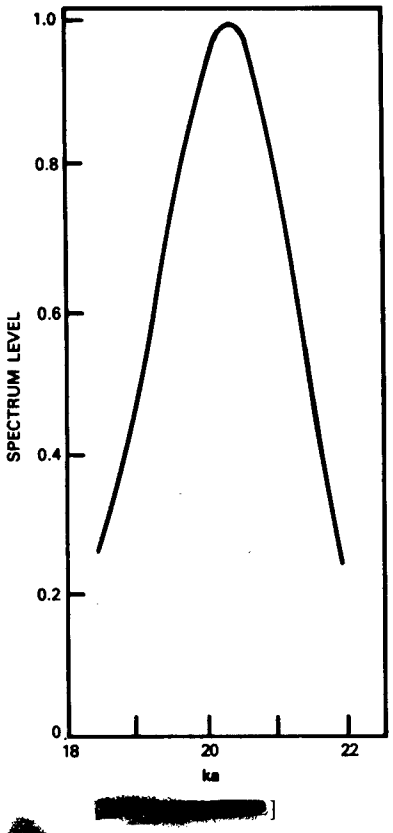

Fig. 21a — The spectrum $|g_r(ka)|$ of the first pulse reflected at an aspect angle of 50° in water

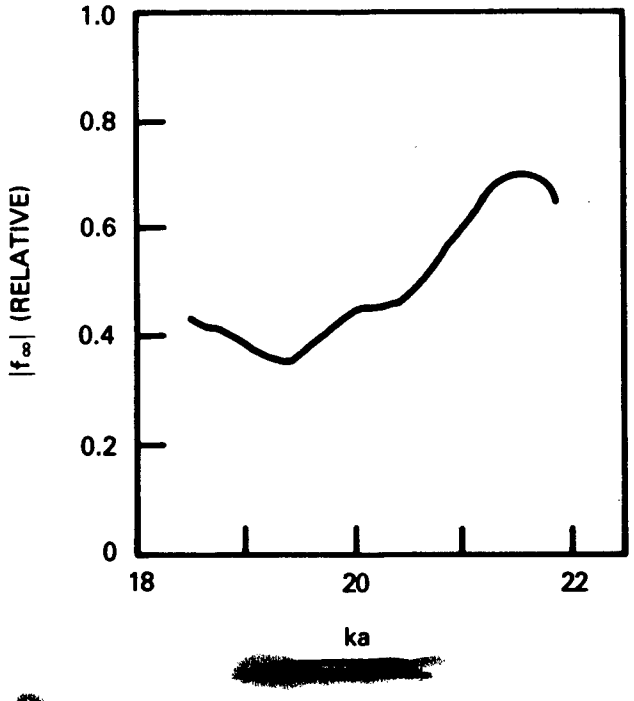

Fig. 21b — The form function resulting from deconvolution using the spectrum of only the first pulse reflected at an aspect angle of 50° in water

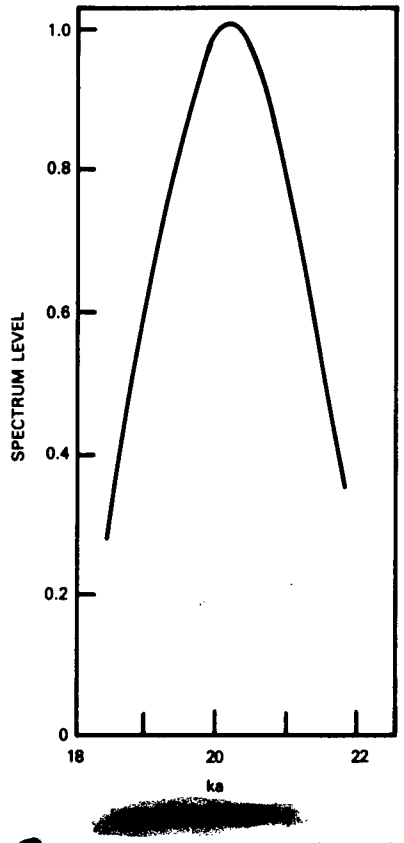

Fig. 22a — The spectrum $|g_r(ka)|$ of the first pulse reflected at an aspect angle of 60° in water

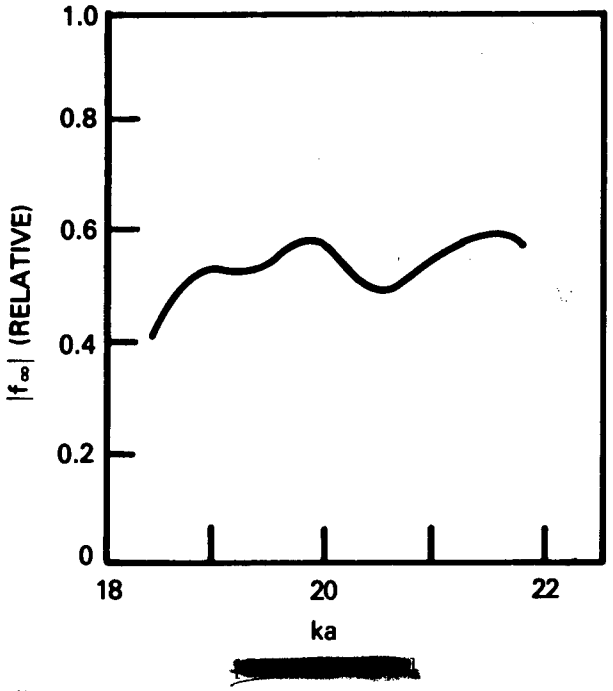

Fig. 22b — The form function resulting from deconvolution using the spectrum of only the first pulse reflected at an aspect angle of 60° in water

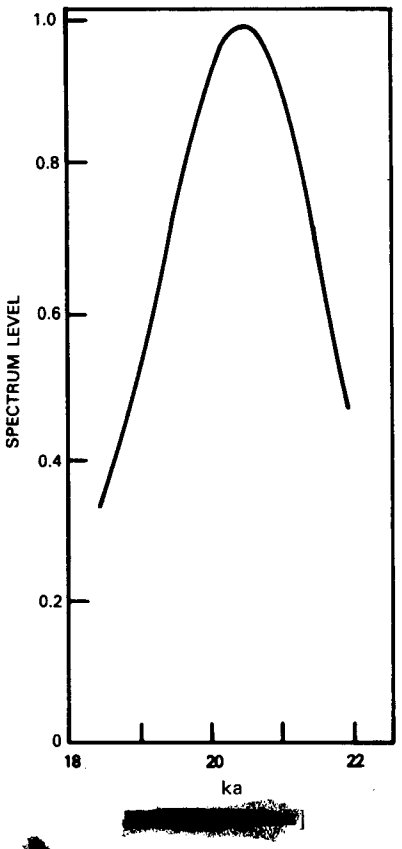

Fig. 23a — The spectrum $|g_r(ka)|$ of the first pulse reflected an as aspect angle of 80° in water

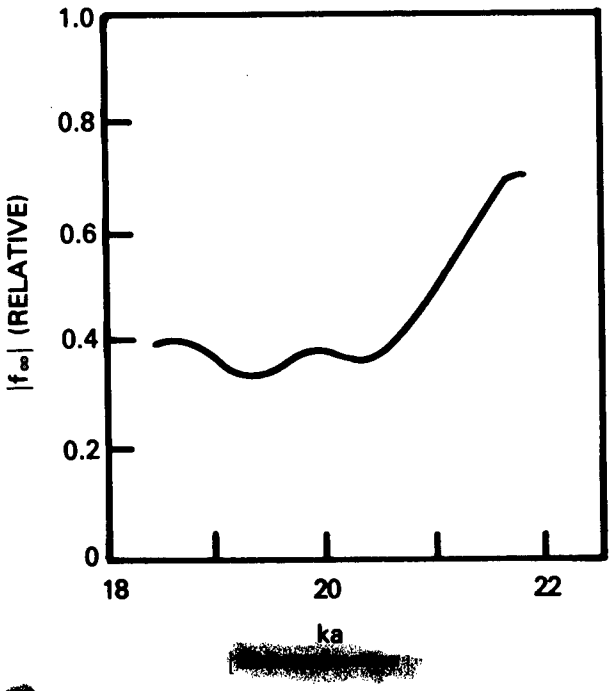

Fig. 23b — The form function resulting from deconvolution using the spectrum of only the first pulse reflected at an aspect angle of 80° in water

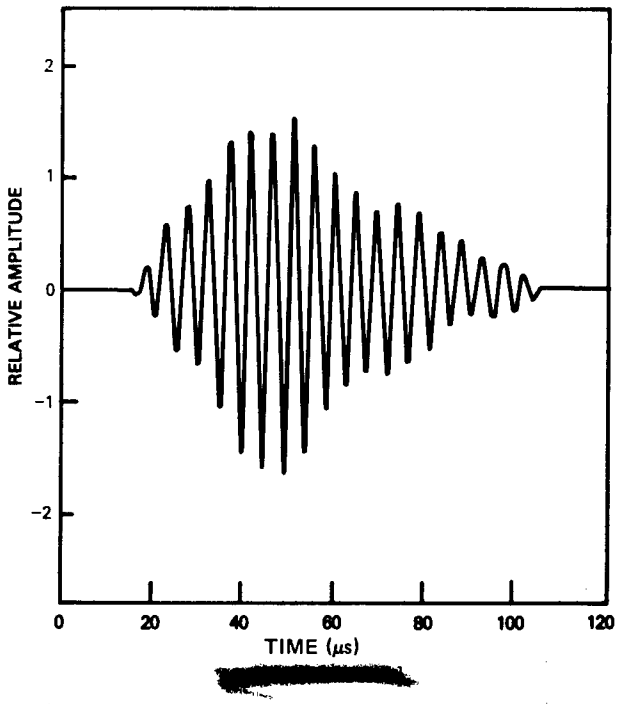

Fig. 24 — The first reflected pulse $p_r(t)$ measured at an aspect angle of 30° in water when the pulse in Fig. 13 is incident on the submarine model. Figure 19a shows the spectrum of this pulse

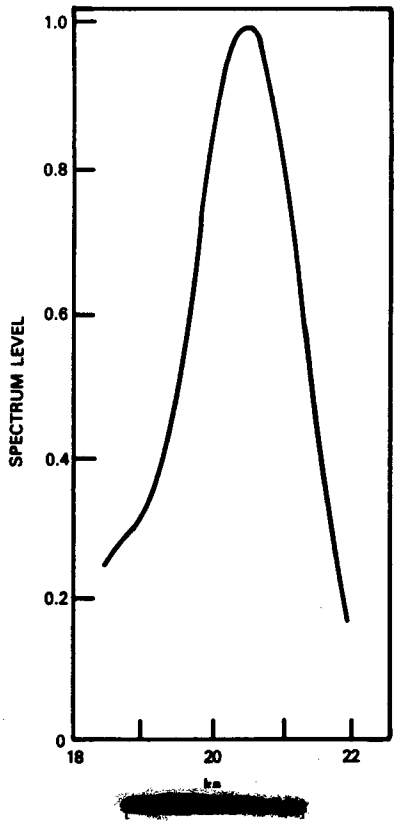

Fig. 25a — The spectrum $|g_r(ka)|$ of the first pulse reflected at an aspect angle of 30° in water in a later experiment intended to duplicate the conditions that resulted in Fig. 19a

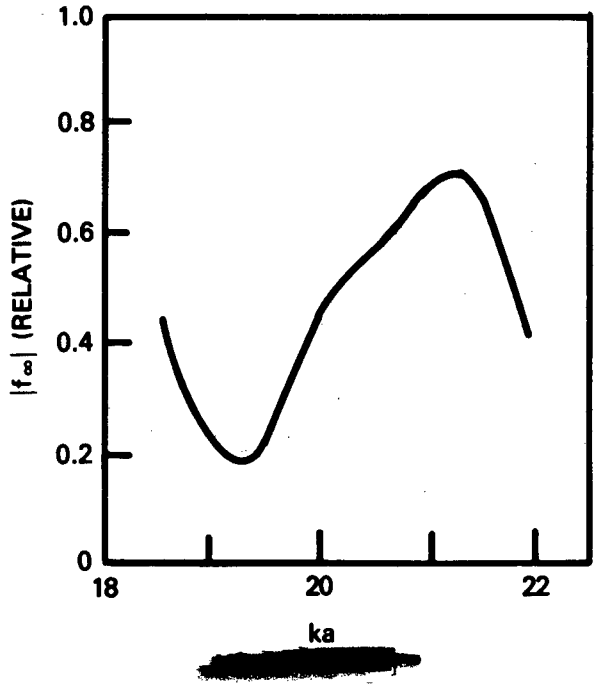

Fig. 25b — The form function resulting from deconvolution using the spectrum of only the first pulse reflected at an aspect angle of 30° in water in a later experiment intended to duplicate the conditions that resulted in Fig. 19b

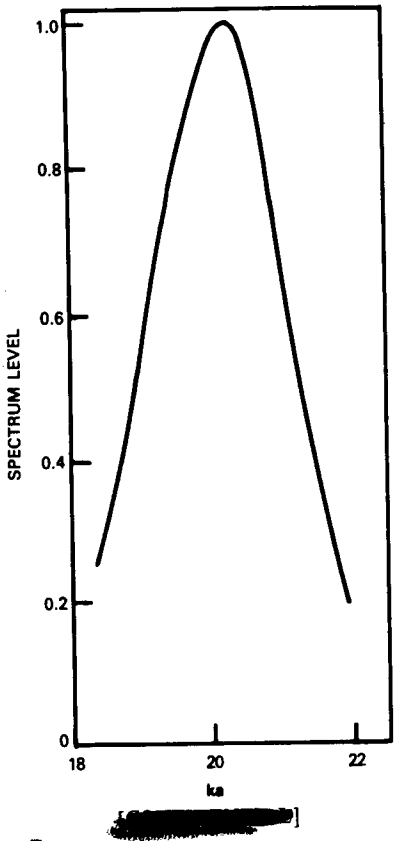

Fig. 26a — The spectrum $|g_r(ka)|$ of the first pulse reflected at an aspect angle of 40° in water in a later experiment intended to duplicate the conditions that resulted in Fig. 20a

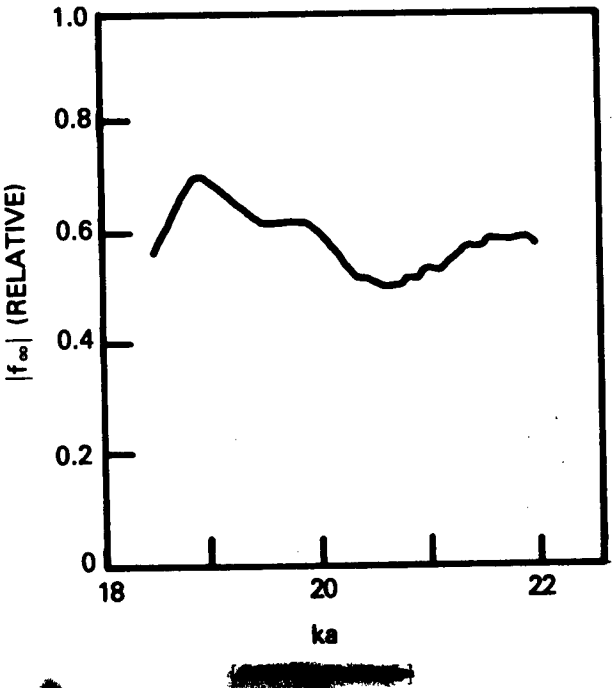

Fig. 26b — The form function resulting from deconvolution using the spectrum of only the first pulse reflected at an aspect angle of 40° in water in a later experiment intended to duplicate the conditions that resulted in Fig. 20b

For this purpose a 1/300-scale model of a Soviet SSGN Charlie (Fig. 27) was used. A photograph of the model disassembled and partially assembled is shown in Fig. 28. The forward section of the inner (pressure) hull is not to be taken as the authentic or most likely configuration to be expected in real life. During the experiment, the inner hull was air filled, and the space between the inner and outer hulls, as well as the space in the sail and the tail sections, was filled with water. One side of the outer hull was left bare, and the other side was coated with an echo-reduction coating that afforded approximately 17 dB echo reduction at 6 MHz (real frequency), which would be equivalent to a frequency of 20 kHz for a full-scale Soviet Charlie submarine.

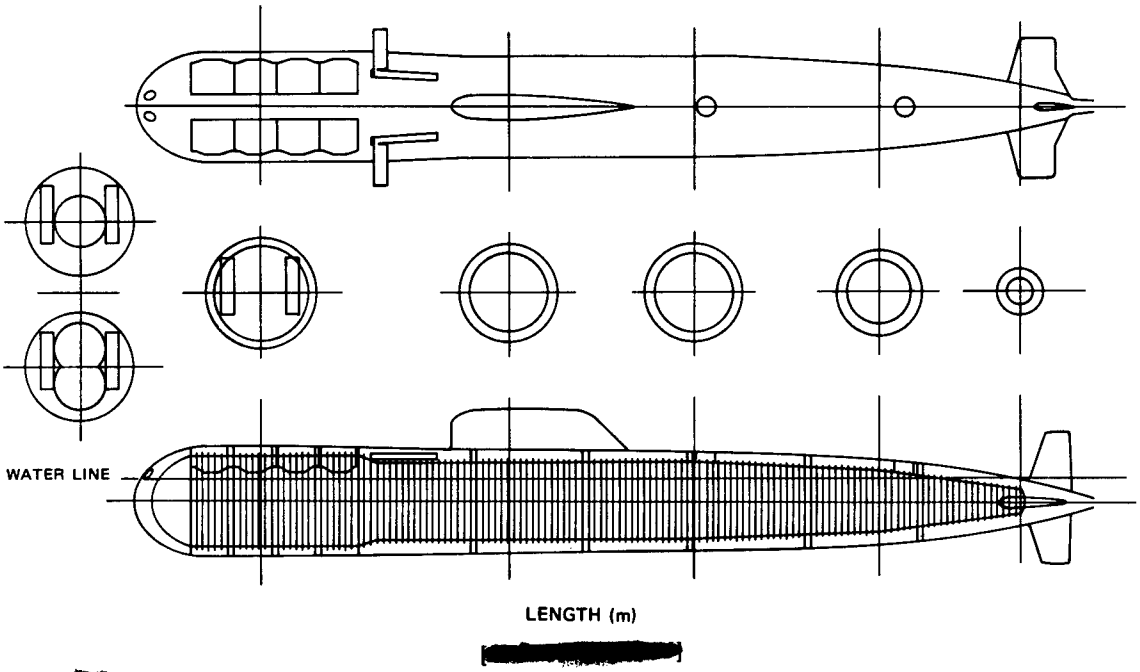

Fig. 27 — Estimated pressure-hull configuration of a Soviet Charlie-class submarine. Three possible choices are shown at the left for the bow crossection

The center frequency of the pulses used in these experiments was 412.5 kHz, corresponding to an equivalent-full-scale frequency of 1375 Hz and a *ka* of 27.5. At that frequency the same coating afforded very little echo reduction. It did, however, significantly modify the shape of the reflected echo; hence the test was considered adequate for examining form-function behavior. The recording of the incident pulse has unfortunately been lost. However, the incident-pulse Fourier transform is shown in Fig. 29 and is unspectacular enough that reconstruction of the incident pulse itself is not warranted.

The entire backscattered reflected pulse, at a target aspect angle of 107.5° from the bow, is shown in Fig. 30a, for which the Fourier transforms is given in Fig. 30b. Deconvolution of the reflected and incident transform result in the form function in Fig. 30c for the uncoated side of the target. Using only the first part of the reflected echo shown in Fig. 31a, whose transform is given in Fig. 31b, results in the form functions shown in Fig. 31c. Again a regular smooth slowly undulating curve results.

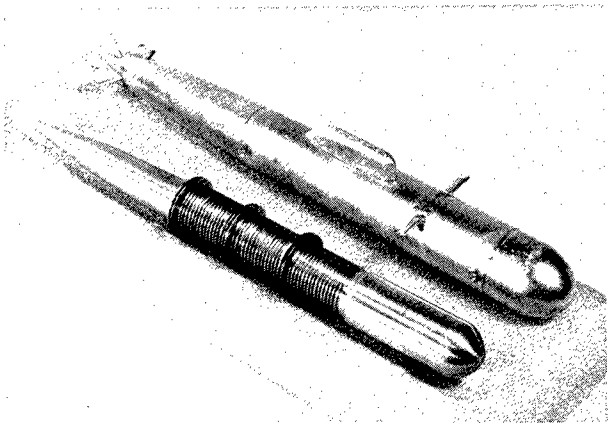

(a) Assembled outer hull (top) and inner pressure hull with some ribs and frames (bottom)

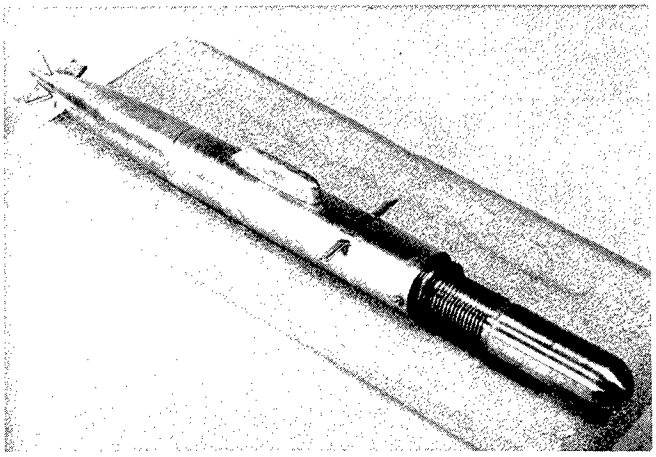

(b) Pressure hull partially inserted into inner hull

Fig. 28 — Two views of a 1/300-scale Soviet Charlie-class submarine model

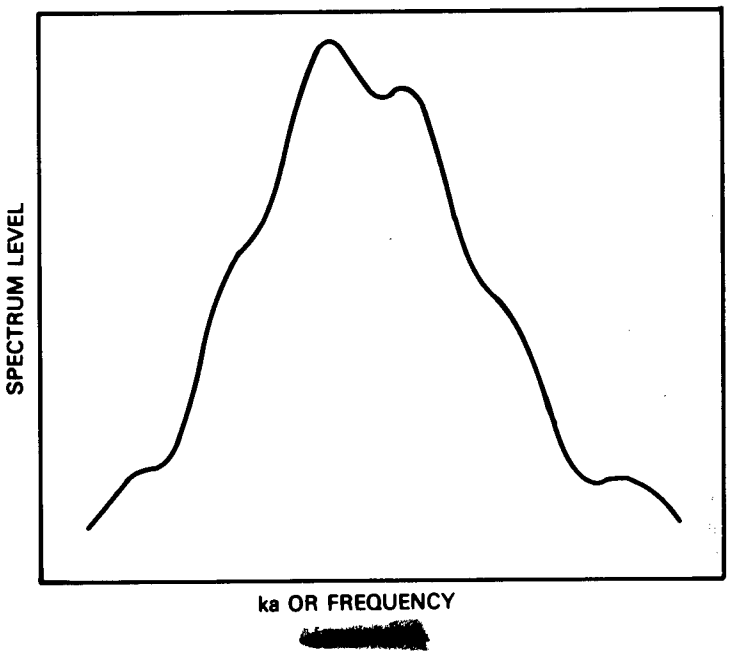

Fig. 29 — The spectrum $|g_i(ka)|$ of the incident pulse used in echo experiments on the Charlie-class-submarine model in water at a frequency of approximately 1.4 kHz

A similar experiment was conducted at the same target aspect angle of 107.5° from the bow on the opposite (coated) side of the model target. The sequence of entire target echo, its spectrum, and its form function is shown in Figs. 32a, 32b, and 32c. The resultant form function from this process is again observed to be irregular and definitely not smooth. The sequence of the first part of the backscattered echo, its spectrum, and the deconvolution with the spectrum of the incident pulse, which results in the form function, is shown in Figs. 33a, 33b and 33c. Again, the form function is smooth and slowly undulating. Comparison of Figs. 30a and 32a shows that the peak pulse amplitude has been reduced by the coating applied to the model. However, comparison of Figs. 31a and 33a shows that the first part of the echo was not reduced but is significantly larger from the coated side.

These studies were not meant to be a complete exploration of the concepts involved but rather to be an examination by selected experiments to examine the idea of first-pulse deconvolution and its production of a relatively smooth and stable (form) function that might be used to detect and identify potentially hostile submarines such as Soviet submarines with their characteristic double-hull construction and almost universal echo-reduction coating It would have been most desirable to make a more thorough examination of frequency regions where echo-reduction effectiveness of coatings was higher. Although more data were taken than presented here, many more data are necessary to examine the stability and characteristics of the form function derived from first-pulse echoes to maximize or optimize their usefulness. These results, however, are sufficiently extensive and intensive to demonstrate that the concept has potential use in submarine detection and probably identification and may hold promise for even a much broader class of reflectors of Navy interest, such as mines or other man-made objects in the sea.

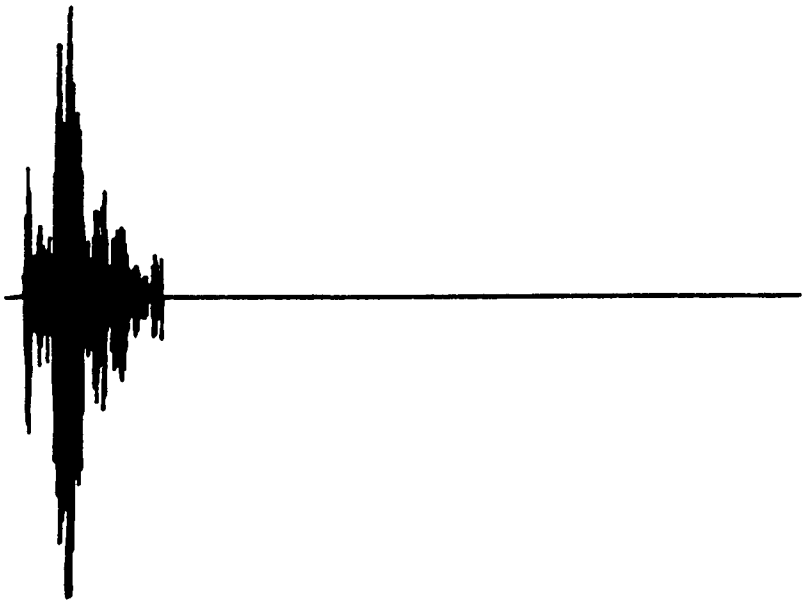

Fig. 30a — The entire reflected pulse at an aspect angle of 107.5° from the bow of the submarine model shown in Fig. 28, reflected in water from the side of the model with no anechoic coating

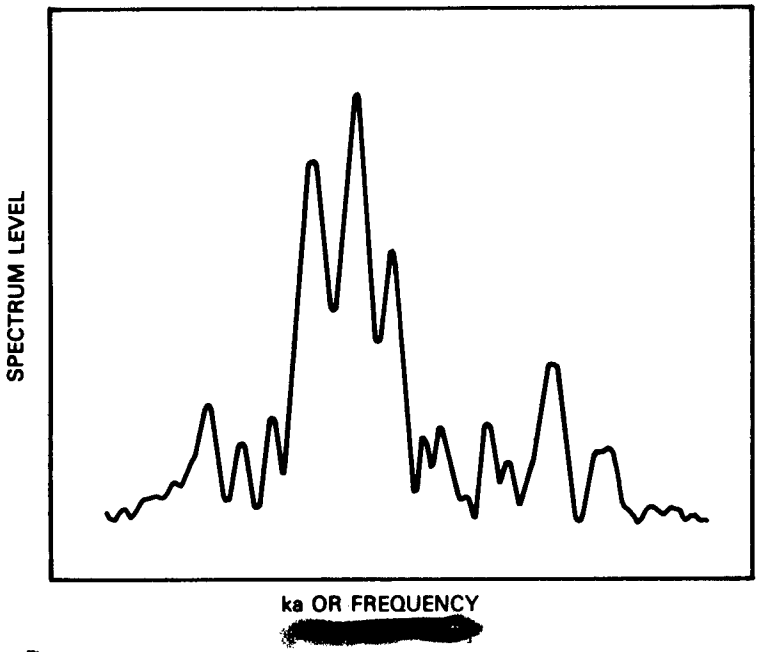

Fig. 30b — The spectrum $|g_r(ka)|$ of the entire reflected pulse at an aspect angle of 107.5° shown in Fig. 30a (no coating on the model)

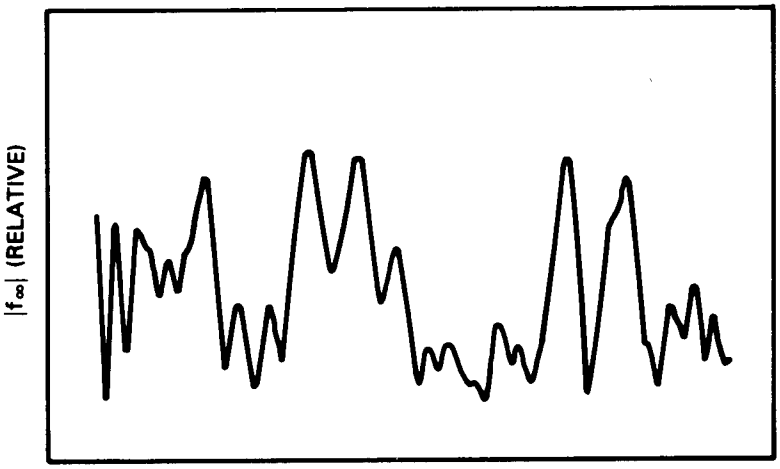

Fig. 30c — The form function resulting from deconvolution using the spectrum of the entire reflected pulse at an aspect angle of 107.5° from the uncoated side of the model

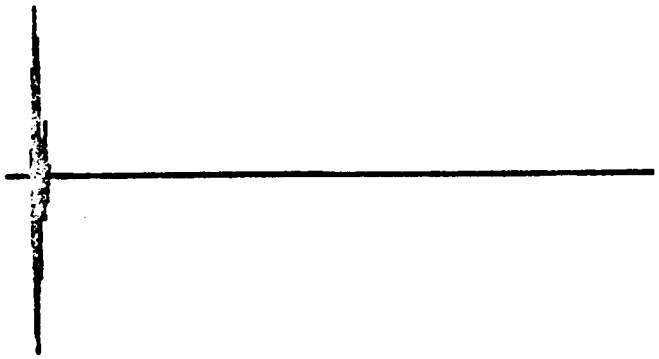

Fig. 31a — The first reflected pulse at an aspect angle of 107.5° in water from the uncoated side of the model shown in Fig. 28

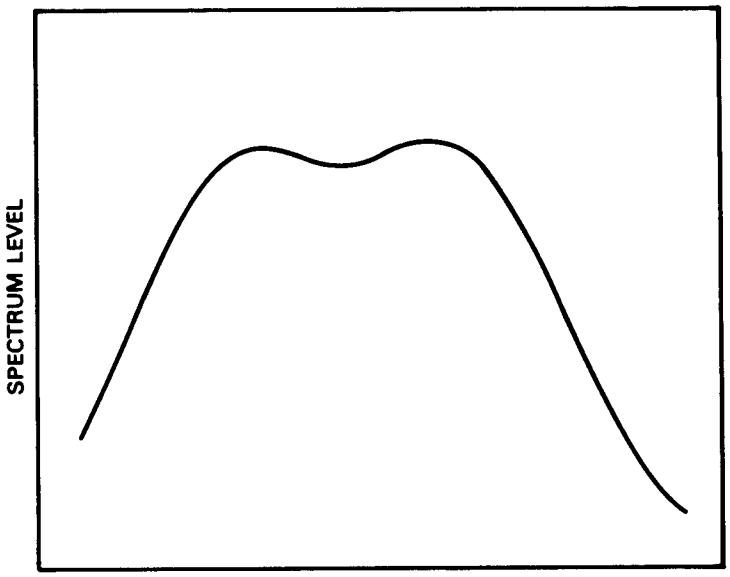

Fig. 31b — The spectrum $|g_r(ka)|$ of the first reflected pulse at an aspect angle of 107.5° from the uncoated side of the model

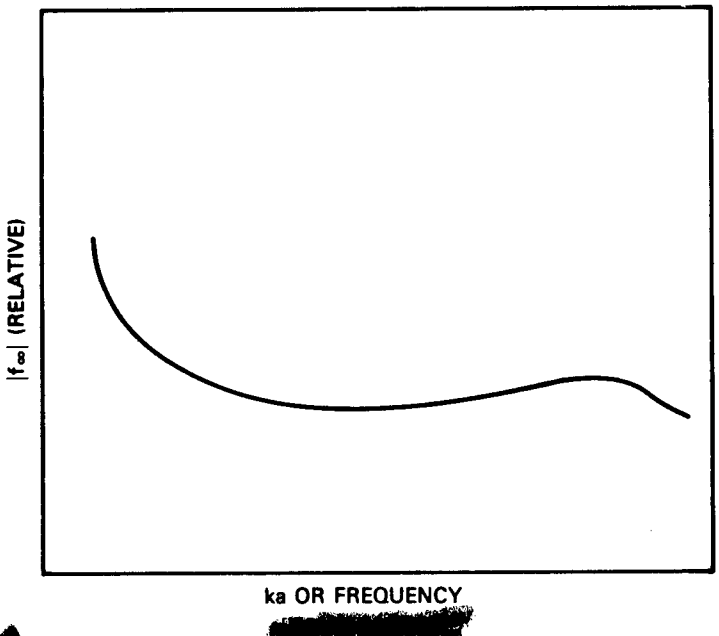

Fig. 31c — The form function resulting from deconvolution using the spectrum of only the first pulse reflected at an aspect angle of 107.5° and the spectrum of the incident pulse (Fig. 29)

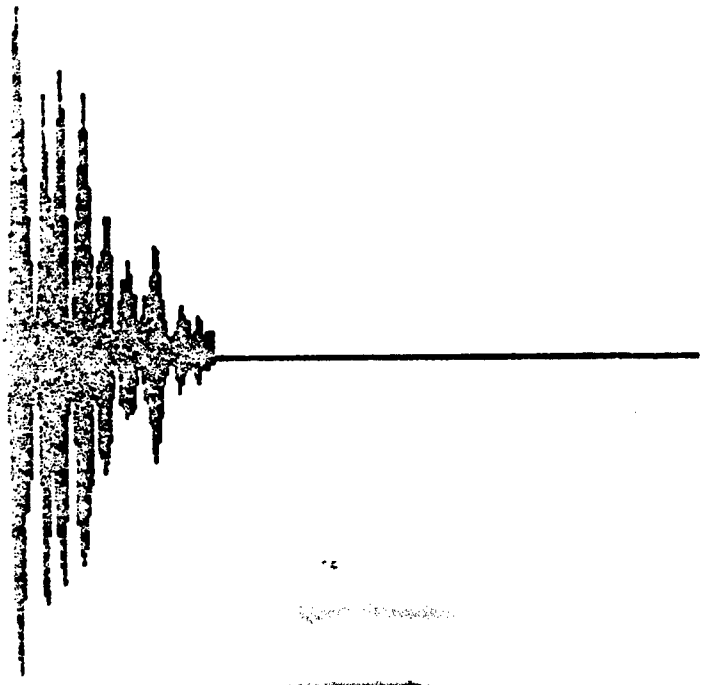

Fig. 32a — The entire reflected pulse at an aspect angle of 107.5° in water from the coated side of the model shown in Fig. 28

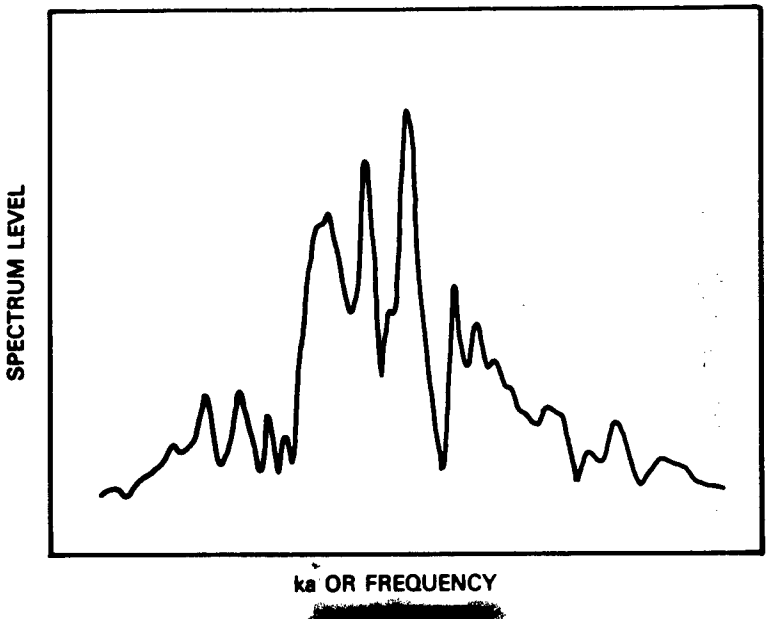

Fig. 32b — The spectrum of the entire reflected pulse at an aspect angle of 107.5° shown in Fig. 32a (coating on the model)

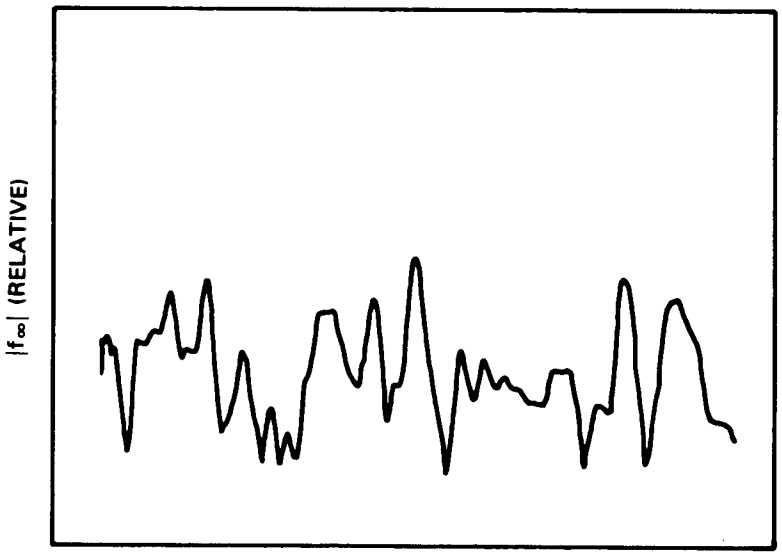

Fig. 32c — The form function resulting from deconvolution using the spectrum of the entire reflected pulse at an aspect angle of 107.5° from the coated side of the model

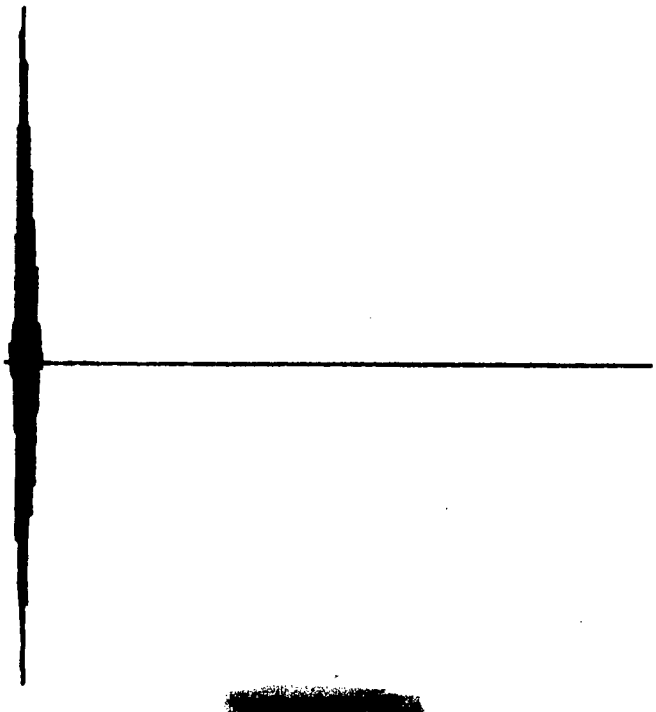

Fig. 33a — The first reflected pulse at an aspect angle of 107.5° in water from the coated side of the model shown in Fig. 28

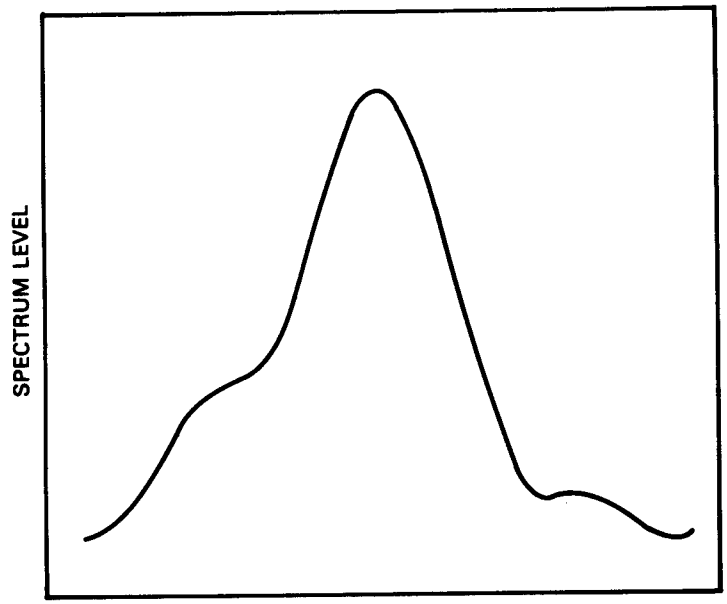

Fig. 33b — The spectrum $|g_r(ka)|$ of the first reflected pulse at an aspect angle of 107.5° from the coated side of the model

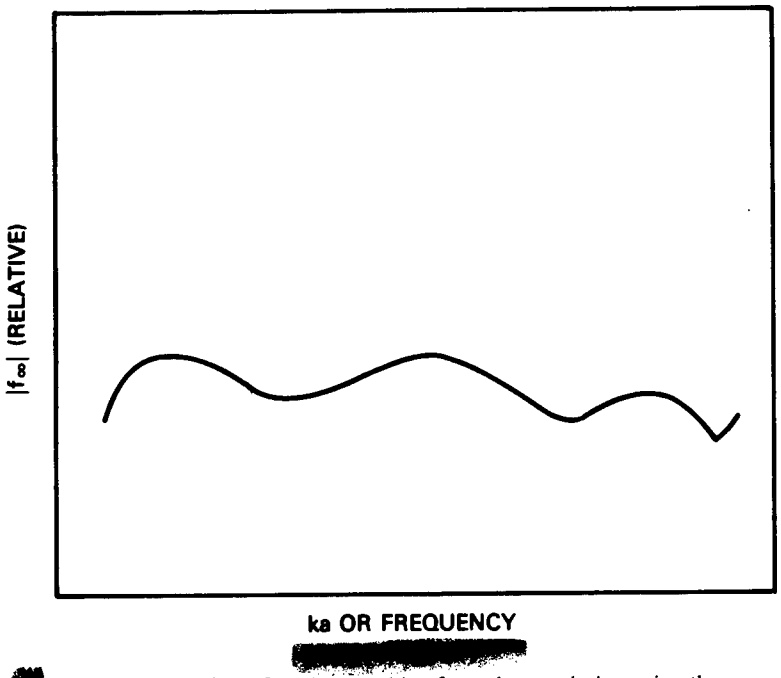

Fig. 33c — The form function resulting from deconvolution using the spectrum of only the first pulse reflected at an aspect angle of 107.5° from the coated side of the model

ACKNOWLEDGMENTS

(U) The material for this report was accumulated over a considerable period of time; therefore the work of others is reflected in this report and is acknowledged with thanks: Mr. Richard Vogt conducted many of the measurements, Dr. Louis Dragonette coordinated measurements and calculations and was ever ready with helpful discussions, Dr. Lawrence Flax contributed to analytical efforts, and Roberta Hopkins prepared the manuscript.

REFERENCES

1. L.R. Dragonette, R.H. Vogt, L. Flax, and W.G. Neubauer, J. Acoust. Soc. Am. *55*, 1130-1137 (1974).

2. R.H. Ferris, B.G. Hurdle, R.J. Mackey, Jr., and K.P. Thompson, NRL Report 4629 ([redacted]), November 30, 1955.

3. W.G. Neubauer, L.R. Dragonette, and R.H. Vogt, NRL Report 7893 ([redacted]), June 12, 1975.

[redacted]

UNCLASSIFIED

UNCLASSIFIED

[redacted]

THE NAVAL RESEARCH LABORATORY IS AN ACTIVITY OF THE OFFICE OF NAVAL RESEARCH